

Nrf3 promotes the proliferation and migration of triple-negative breast cancer by activating PI3K/AKT/mTOR and epithelial-mesenchymal transition

WAN-MENG CHEN, QING-YONG HU, WEI HOU, MENG-WEI CHEN, YA-HUI CHEN and JIAN-CAI TANG

Department of Biochemistry, Institute of Basic Medicine and Forensics Medicine,
North Sichuan Medical College, Nanchong, Sichuan 637000, P.R. China

Received April 21, 2023; Accepted July 31, 2023

DOI: 10.3892/ol.2023.14030

Abstract. Nuclear factor erythroid 2-related factor 3 (Nrf3) is increasingly implicated in multiple types of cancer; however, its function in triple-negative breast cancer (TNBC) remains unclear. This study aimed to examine the role of Nrf3 in TNBC. Compared with adjacent normal tissues, TNBC tissues expressed higher levels of Nrf3, and its expression was negatively correlated with survival time. Additionally, Nrf3 knockdown reduced the proliferation and migration of TNBC cells, whereas overexpression of Nrf3 had the opposite effects *in vitro* and *in vivo*. Moreover, functional enrichment of TNBC cells overexpressing Nrf3 allowed for the identification of numerous genes and pathways that were altered following Nrf3 overexpression. Further study showed that overexpression of Nrf3 activated the PI3K/AKT/mTOR signaling pathway and regulated the expression of proteins associated with epithelial-mesenchymal transition. Nrf3 was found to directly bind to p110 α promoter regions, as evidenced by luciferase reporter and chromatin immunoprecipitation assays. Furthermore, PI3K inhibitors partially decreased the proliferation and migration of the Nrf3 overexpressing TNBC cells. In conclusion, Nrf3 enhances cellular proliferation and migration by activating PI3K/AKT/mTOR signaling pathways, highlighting a novel therapeutic target for TNBC.

Introduction

Amongst all cancers diagnosed in women, breast cancer accounts for 11.7% of cases and is the leading cause of cancer-associated death in women worldwide (1). Breast

cancer can be classified into four subtypes, depending on the receptor status: Luminal A, luminal B, HER2 positive, and triple-negative (2). The incidence of triple-negative breast cancer (TNBC) is estimated to be 15-20% of all breast cancer cases (3), and is characterized by a high rate of early recurrence and distant metastases compared with other types of breast cancer (4). Owing to the lack of expression of estrogen receptor (ER), progesterone receptor (PgR), and *ERBB2* (*HER2*), the current treatment methods for TNBC primarily include surgery, radiotherapy, and chemotherapy (5). Although significant progress has been achieved in the treatment modalities and management strategies, the survival rates of patients have not significantly improved. Thus, further investigation of the underlying molecular mechanisms and biological behaviors of TNBC, which will provide a solid foundation for developing new therapeutic strategies, is vital.

Nuclear factor erythroid-derived 2-like 3 (Nrf3), also known as NFE2L3, first identified in 1999, is a member of the Cap'n'Collar (CNC) family, which is comprised mainly of Nrf1, Nrf2, BACH1, and BACH2 (6). The CNC family is similar to leucine zippers in basic regions, indicating their function may be similar (7). Recent research on Nrf1 and Nrf2 has attracted notable attention, showing that the ability of Nrf2 (8,9) to mediate metabolic reprogramming and increase antioxidant capacity underlies the malignant behaviors of NRF2-activated cancer cells, and that Nrf1 (10) protects cancer cells from proteotoxicity induced by anticancer proteasome inhibitors. However, there are few reports on Nrf3, partly due to a lack of evident abnormalities, such as in gross anatomy and multiple blood parameters in Nrf3-deficient mice (11). Nonetheless, the role of Nrf3 differs from that of other CNC family members, and is similar to the definitive role of Nrf2 in oxidative stress (12). Nrf1 maintains protein stability by maintaining proteasome gene expression (13). Nrf3 is implicated in multiple cellular processes, such as tumorigenesis (14), inflammation, wound healing (15), and stem cell differentiation (16). Consequently, Nrf3 has been identified as a critical component of multiple types of cancer, including colon cancer (17) and pancreatic cancer (18). Nrf3 may be involved in tumor growth and invasion via the β -catenin/TCF4 signaling pathway, which degrades the tumor suppressor p53 and Rb in a ubiquitin-independent manner (19). Nrf3 also affects the cell cycle via the

Correspondence to: Dr Jian-Cai Tang, Department of Biochemistry, Institute of Basic Medicine and Forensics Medicine, North Sichuan Medical College, 234 Fu Jiang Road, Shun Qing, Nanchong, Sichuan 637000, P.R. China
E-mail: tangjiancai@nsmc.edu.cn

Key words: nuclear factor erythroid 2-related factor 3, triple-negative breast cancer, proliferation and migration, PI3K/Akt/mTOR, epithelial-mesenchymal transition

NF- κ B-DUX4-CDK1 signaling pathway (17). Additionally, Nrf3 knockdown in hepatocellular carcinoma cells resulted in increased migration and epithelial-mesenchymal transition (EMT) (20). These studies suggest a potential involvement of Nrf3 in tumorigenesis. However, there is insufficient evidence to explain how Nrf3 plays a role in TNBC development.

As a group of plasma membrane-associated lipid kinases, three classes of PI3K exist: Class I, class II, and class III, each characterized by their unique structure and specific substrate. The class I PI3Ks are classified as class A and class B. A class IA PI3K has two subunits: A regulatory subunit (P85) and a catalytic subunit (P110). The catalytic subunits in class IA PI3K are divided into three types: p110 α , p110 β , and p110 δ , which correspond to the genes PIK3CA, PIK3CB, and PIK3CD, respectively (21). Among these PI3K genes, breast cancer is associated with p110 abnormal activation. The PI3K/AKT/mTOR cascade, one of the primary signaling pathways of tyrosine kinases, controls several cellular functions, such as proliferation and protein synthesis. Additionally, the overactivation of the PI3K/AKT/mTOR signaling pathway results in various biological changes to breast cancer cells (22), and P110 α enhances the proliferation and migratory ability of breast cancer cells by activating the EMT signaling pathway (23,24).

In the present study, TNBC specimens showed higher Nrf3 expression compared with other types of breast cancer tissues and adjacent noncancerous tissues, and its expression was negatively associated with survival. Furthermore, Nrf3 knockdown reduced cell proliferation and migration *in vitro* and *in vivo*. In comparison, overexpression of Nrf3 had the opposite effect. Moreover, the results showed that Nrf3 increased P110 α , p-AKT, and p-mTOR expression and regulated the expression of EMT-related proteins. The findings suggest that Nrf3 may enhance the proliferation and migration of TNBC by modulating PI3K/AKT/mTOR signaling, thereby highlighting a novel therapeutic target for the management of TNBC.

Materials and methods

Clinical samples and bioinformatics analysis. Breast cancer and adjacent cancer tissues (n=105) were harvested at the Affiliated Hospital of North Sichuan Medical College between October 2018 and October 2021. It was confirmed that all cancer cases were breast cancer, and the subtypes were also confirmed. There were 35 TNBC cases, 35 Her2⁺ cases, and 35 Lumina cases. The Cancer Genome Atlas (TCGA) and GTEX were used to examine Nrf3 expression in breast cancer and normal tissues. Preoperative radiotherapy and chemotherapy were not administered to any patients. Related clinical data were collected. All patients provided informed consent for the use of clinical research materials.

Immunohistochemistry. Tissues were first fixed at room temperature for 48 h in 4% formaldehyde solution, dehydrated using an increasing series of alcohol solutions, deparaffinized using a hyaline agent, embedded in paraffin and finally sectioned into 4- μ M thick sections and stored at 4°C. After sectioning, antigen retrieval was performed using sodium

citrate for 25 min at 100°C in a water bath, followed by drying, dewaxing and hydration using a decreasing series of alcohol solutions. The sections were immersed in 3% hydrogen peroxide for 15 min to quench endogenous peroxidase activity and immediately incubated at 4°C overnight with primary antibodies (rabbit anti-Nrf3 antibody; cat. no. PA5-99083; 1:50; Thermo Fisher Scientific, Inc.). The following day, the samples were incubated with the horseradish peroxidase-conjugated secondary antibodies (cat. no. AB0101; Abways Technology) for 1 h at 37°C. The slides were then stained with DAB (DAB Plus Kit from MXB Biotechnologies) solution for 2 min at room temperature, counterstained with hematoxylin for 30 sec and dried for blocking. Two experienced pathologists evaluated the results according to the percentage of positively stained tumor cells and staining intensity.

Positive staining degree was classified as 0, <10%; 1, 10-20%; 2, 21-50%; and 3, >50%. The staining intensity was graded as follows: 0, no staining; 1, weak staining; 2, moderate staining; and 3, strong staining. To calculate the final scores, the score for the percentage stained was added to the score for the staining intensity. The final scores were stratified as ≥ 6 and <6, indicating high and low expression, respectively.

Cell culture and lentivirus transfection. MDA-MB-231 and MDA-MB-468 (triple-negative breast cancer cell lines) were provided by the National Collection of Authenticated Cell Cultures. The PI3K pathway inhibitor, LY294002 (Selleck Chemicals), was purchased in powder form, dissolved to 100 mM using DMSO, and then stored at -80°C. The Nrf3 lentiviral vector (sc-404543-LAC) and negative control were obtained from Santa Cruz Biotechnology, Inc. Two shRNA target sequences for Nrf3 were designed and inserted into the pLKO.1 vector. shRNA plasmids were transfected with lentiviruses to generate a recombinant lentivirus. The Nrf3 shRNA interference target sequences were based on our previous study (25).

A total of 2x10⁵ MDA-MB-231 or MDA-MB-468 cells were seeded in each well, and cultured to 40% confluency. In addition to the complete medium, lentiviral particles were added at a final concentration of polybrene (5 μ g/ml). After mixing, the original medium was replaced, and infection was allowed for 24 h. After 24 h, the medium was replaced and puromycin hydrochloride was added to allow for screening for 48 h. The effect of overexpression and knockdown of Nrf3 was determined using western blotting.

Western blotting. Cells were lysed using western & IP lysis buffer (cat. no. P0013; Beyotime Institute of Biotechnology). The proteins were loaded on a 10% SDS gel, resolved using SDS-PAGE, and then transferred to PVDF membranes. Membranes were blocked in TBST with 5% skimmed milk. Next, membranes were blocked with primary antibodies at 4°C overnight, including anti-Nrf3 (cat. no. PA5-102015; 1:1,000; Thermo Fisher Scientific, Inc.), anti-PI3K p110 α (cat. no. 4249; 1:1,000; Cell Signaling Technology, Inc.), anti-phospho-Akt (S473) (cat. no. 4060; 1:1,000; Cell Signaling Technology, Inc.), rabbit anti-phospho-Akt (Thr308) (cat. no. 13038; 1:1,000; Cell Signaling Technology, Inc.), anti-Akt (cat. no. 9272; 1:1,000; Cell Signaling Technology, Inc.), anti-phospho-mTOR (Ser2448) (cat. no. 5536; 1:1,000;

Cell Signaling Technology, Inc.), anti-mTOR (cat. no. 2972; 1:1,000; Cell Signaling Technology, Inc.), anti-E-cadherin (cat. no. 20874-1-AP; 1:1,000; ProteinTech Group, Inc.), anti-N-cadherin (cat. no. 22018-1-AP; 1:1,000; ProteinTech Group, Inc.), anti-Vimentin (cat. no. 10366-1-AP; 1:1,000; ProteinTech Group, Inc.), anti-MMP-3 (cat. no. 17873-1-AP; 1:1,000; ProteinTech Group, Inc.), anti-MMP-9 (cat. no. 10375-2-AP; 1:1,000; ProteinTech Group, Inc.) and anti-GAPDH (cat. no. AB0036; 1:5,000; Abways Technology) antibody. The following day, the membranes were incubated with the relevant secondary antibody. Between and after incubation with the antibodies, membranes were washed with TBST. Signals were visualized using Immobilon ECL Ultra Western HRP (cat. no. WBULS0100, MilliporeSigma). The results were analysed using a ChemiDoc XRS + Gel Imaging System (Bio-Rad Laboratories, Inc).

Transcriptome sequencing and analysis. MDA-MB-231 and MDA-MB-231/Nrf3 cells were collected and prepared for three paired biological replications. The samples were sent to oebiotech company (<https://www.oebiotech.com/>) for sequencing. Total RNA was extracted using the mirVana miRNA Isolation Kit (cat. no. 1561; Ambion; Thermo Fisher Scientific, Inc.) following the manufacturer's protocols. RNA integrity was evaluated using the Agilent 2100 Bioanalyzer (Agilent Technologies, Inc.). The samples with RNA Integrity Number (RIN) ≥ 7 were subjected to the subsequent analysis. The libraries were constructed using TruSeq Stranded mRNA LTSample Prep Kit (15 cycles; cat. no. RS-122-2103; Illumina, Inc.) according to the manufacturer's instructions. The purified library products were evaluated using the Agilent 2200 Tape Station and Qubit[®] 2.0 (Life Technologies; Thermo Fisher Scientific, Inc.) and then diluted to 10 pM for cluster generation in situ on the pair-end flow cell followed by HiSeq2500 sequencing (2x150 bp). Raw data (raw reads) of fastq format were firstly processed using Trimmomatic (version 0.36) (26) and the low quality reads were removed to obtain the clean reads. The clean reads were mapped to the human genome (GRCh38) using HISAT2.2.1 (27). The fragments per kilobase of transcript per million mapped reads of each gene were calculated using Cufflinks 2.2.1 (28) and the read counts of each gene were obtained by HTSeq-count version 2.0.4 (29) Differential expression analysis was performed using the DESeq (2012) R package (30). $P < 0.05$ and fold-change > 2 and < 0.5 were set as the thresholds for significant differential expression. Hierarchical cluster analysis of differentially expressed genes was performed to demonstrate the expression pattern of genes in different groups. Gene set variation analysis (GSVA 1.24.2) (R package) (31) was utilized to perform GSVA. The gene set 'hall.v7.0.symbols.gmt' was selected as the reference gene set. $P < 0.05$ was considered to indicate a statistically significant difference. The transcriptome raw data has been deposited in the Sequence Read Archive database (<https://www.ncbi.nlm.nih.gov/sra>; submission no. PRJNA965920).

Reverse transcription-quantitative PCR (RT-qPCR). Total RNA was isolated from MDA-MB-231 cells using TRIzol[®]. The RNA was converted to cDNA using a RevertAid First Strand cDNA Synthesis Kit according to the manufacturer's protocol. qPCR was performed on a CFX Connect Real-Time

PCR Detection System and SuperRealPreMix Plus SYBR Green. Based on the 2^{ΔΔC_q} method (32), the relative RNA expression was calculated. Table SI displays the detailed primer sequences included in this study. The thermocycling conditions were as follows: Initial denaturation at 94°C for 2 min, followed by 40 cycles of 94°C for 30 sec, 60°C for 30 sec and 72°C for 30 sec, and then a final extension at 72°C for 10 min.

Cell proliferation and migration assay. CCK-8 experiments (assays obtained from Dojindo Molecular Technologies, Inc.) were used to determine cell proliferation. Approximately 5×10^3 cells per well were plated into a 96-well plate with complete medium and cultured in an incubator. The spectrometric absorbance was determined using a microplate reader at 450 nm. Each experiment was repeated three times.

For migration assays, wound healing, and Transwell assays were used to investigate cell migration. Transwell assays were performed as follows: 5×10^3 cells in 100 μ l serum-free medium was added to the upper chamber of a Transwell insert without Matrigel. Supplemented medium was added to the lower chamber as a chemoattractant. A cotton swab was used to remove the cells on the upper side after 24 h of incubation. A mixture of 4% formaldehyde and 0.1% crystal violet was used to fix and stain migrated cells at room temperature for 20 min. Finally, the number of cells in three independent fields was counted under a brightfield microscope (IX73; Olympus Corporation) (magnification, x100).

For the wound healing assay, 5×10^3 cells per well were added to a six-well plate. Once a confluent monolayer of cells had formed, the monolayer was scratched and imaged after becoming adherent, and then cultured in serum-free medium for a further 24 h. The cells were imaged again in the same location after washing with PBS.

Luciferase reporter assay. Nrf3, a transcript factor, is known to bind antioxidant response element (ARE) sites, with the core sequence of an ARE being 5'-TGACNNGC-3'. The p110 α promoter sequence was loaded to find multiple ARE sites. Thus, Nrf3 may active P110 α by binding ARE sites. siRNA knockdown of Nrf3 expression and pCMV-Nrf3 overexpression vector were purchased from Cyagen Biosciences. The p110 α promoter was cloned into pEZX (-1,000 bp from the transcription initiation site). The resulting full-length reporter plasmid was termed pEZX-1000, which may contain multiple Nrf3-binding sites. The deletion mutation reporters (pEZX-714 and pEZX-418) were generated using this plasmid. Plasmids and siRNAs were transfected into MDA-MB-231 and MDA-MB-468 cells using Lipofectamine 3000 (Invitrogen; Thermo Fisher Scientific, Inc.).

The MDA-MB-231 and MDA-MB-468 cells were seeded in six-well plates and transfected with a p110 α full-length reporter plasmid or deletion mutant promoter plasmid and Nrf3-overexpressing vector, siNrf3, and the negative control vector together with the PGL4.74 TK-Luc reporter. After transfection (48 h later), the cell lysates were prepared. As directed by the manufacturer, Firefly/Renilla luciferase values were determined using a Dual-Luciferase Reporter Assay System (cat. no. E1910; Promega Corporation). A GloMax-96 plate reader (Promega Corporation) was used to measure the luciferase activity.

ChIP. Pierce magnetic ChIP assays were performed using the Pierce Magnetic ChIP Kit (cat. no. 88848; Thermo Fisher Scientific, Inc.) according to the manufacturer's instructions. Immunoprecipitation was performed using chromatin with anti-Nrf3 and a normal rabbit-IgG antibody. ChIP-enriched DNA was amplified and quantified using qPCR. The primer sets at the Nrf3-binding sites for the p110 α promoter were: Primer 1 forward, 5'-AGCAAAGGTCTCCACGAAGT GAG-3' and reverse, 5'-CGCCGCTGTCAGTGGCTAAC-3'; and primer 2 forward, 5'-TCTCTACCCAGCTCGCCTG-3' and reverse, 5'-GATGCGCAAAGAAGCGGAAG-3'.

Animal experiments. The MDA-231, MDA-231/Nrf3, MDA-231/ShNrf3#1, and MDA-231/shNrf3#2 tumor models were established to investigate the role of Nrf3 in the proliferation and metastasis of TNBC. A total of 20 nude female mice were obtained from the Beijing HFK Biotechnology Co., Ltd. and maintained in micro isolator cages to analyze tumor growth. For subcutaneous inoculation, 5x10⁶ cells were resuspended in PBS and injected subcutaneously into 5-week-old mice (100 μ l per mouse); four groups were formed as follows: MDA-231, MDA-231/Nrf3, MDA-231/ShNrf3#1, and MDA-231/shNrf3#2 (5 mice per group). The tumors were measured every 3 days after their initial appearance. The mice were sacrificed 40 days after the inoculation. Recovery experiments were performed as described previously (25). When tumors appeared, the mice were further divided into three groups of mice: MDA-231(DMSO), MDA-231/Nrf3 (DMSO), MDA-231/Nrf3 (LY294002, 20 mg/kg/day) (5 mice per group). Treatment was performed for 14 days, and the mice were sacrificed at the end of treatment by injection of sodium pentobarbital (150 mg/kg).

For metastasis assays, a total of 20 female nude mice provided by Beijing HFK Biotechnology Co., Ltd. PBS was to resuspend 1x10⁷ cells per ml, of which 100 μ l was injected into the tail veins of each mouse. Mice were divided into four groups as follows: MDA-231, MDA-231/Nrf3, MDA-231/ShNrf3#1, and MDA-231/shNrf3#2 (5 mice per group). After 60 days, the mice were sacrificed, lungs were excised and imaged. Subsequently, the lung tissues were fixed in 4% formalin and embedded in paraffin, and then hematoxylin and eosin staining was performed. Mice were maintained in pathogen-free conditions with a controlled temperature (23 \pm 2 $^{\circ}$ C), relative humidity (45-65%) and light/dark cycle (12/12 h) with free access to food and water at all times. All animal procedures were performed in accordance with the North Sichuan Medical College's Animal Care Committee and the guidelines of the Animal Protection Law of the People's Republic of China (2009). All animal experiments were approved by the Affiliated Hospital of North Sichuan Medical College (approval no. 2022033).

Statistical analysis. Data are presented as the mean \pm standard deviation. A one-way ANOVA followed by a post-hoc Tukey's test or a Student's t-test was used to compare differences between ≥ 3 or 2 groups, respectively. The χ^2 test was performed to analyze the relationship between clinical characteristics and Nrf3 expression. P<0.05 was considered to indicate a statistically significant difference. Statistical analysis was performed using IBM SPSS version 23 (IBM Corp.).

Table I. Association between Nrf3 expression and clinico-pathological factors.

Factors	Nrf3 expression, n		P-value
	High ^a	Low ^b	
Age, years			0.618
<50	31	14	
≥ 50	44	16	
Pathological grade			0.096
1	4	0	
2	62	22	
3	9	8	
Tumor size, cm			0.993
<2	36	14	
≥ 2	39	16	
Lymph node metastasis			0.429
Present	26	8	
Absent	49	22	
TNM stage			0.225
I/II	67	29	
III/IV	8	1	

^aScores ≥ 6 , ^bscores <6. Nrf3, nuclear factor erythroid 2-related factor 3.

Results

Nrf3 expression is increased in TNBC, and its expression is negatively associated with survival. Bioinformatics was used to analyze Nrf3 mRNA expression in different types of breast cancer. The findings revealed that Nrf3 expression in patients with TNBC was upregulated compared to its expression in other types of breast cancer and adjacent tissues, based on data obtained from TCGA and GTEX (Fig. 1A-C). According to the Kaplan-Meier survival curves, patients with TNBC expressing high levels of Nrf3 had shorter survival times (Fig. 1D). The correlation between Nrf3 and EMT-related genes was also analyzed; the results are shown in Fig. S1A-D.

A total of 105 patients with breast cancer of different pathological types were examined for expression of Nrf3 in their pathological tissues using immunohistochemistry. Higher expression of Nrf3 was detected in TNBC tissues compared with other types of breast cancer and adjacent tissues (Fig. 1E and F). Analysis of the correlation between clinical characteristics and Nrf3 expression was conducted using a χ^2 test. The score for Nrf3 expression in breast cancer was divided into high expression (scores ≥ 6) and low expression (scores <6). There was no association between Nrf3 expression and age, lymph node metastases, tumor sizes, or TNM stage (Table I).

Overexpression of Nrf3 contributes to the proliferation and migration of TNBC. TNBC cell lines stably overexpressing Nrf3 or with Nrf3 expression knocked down were constructed to determine whether Nrf3 played a role in the proliferation and migration of breast cancer cells.

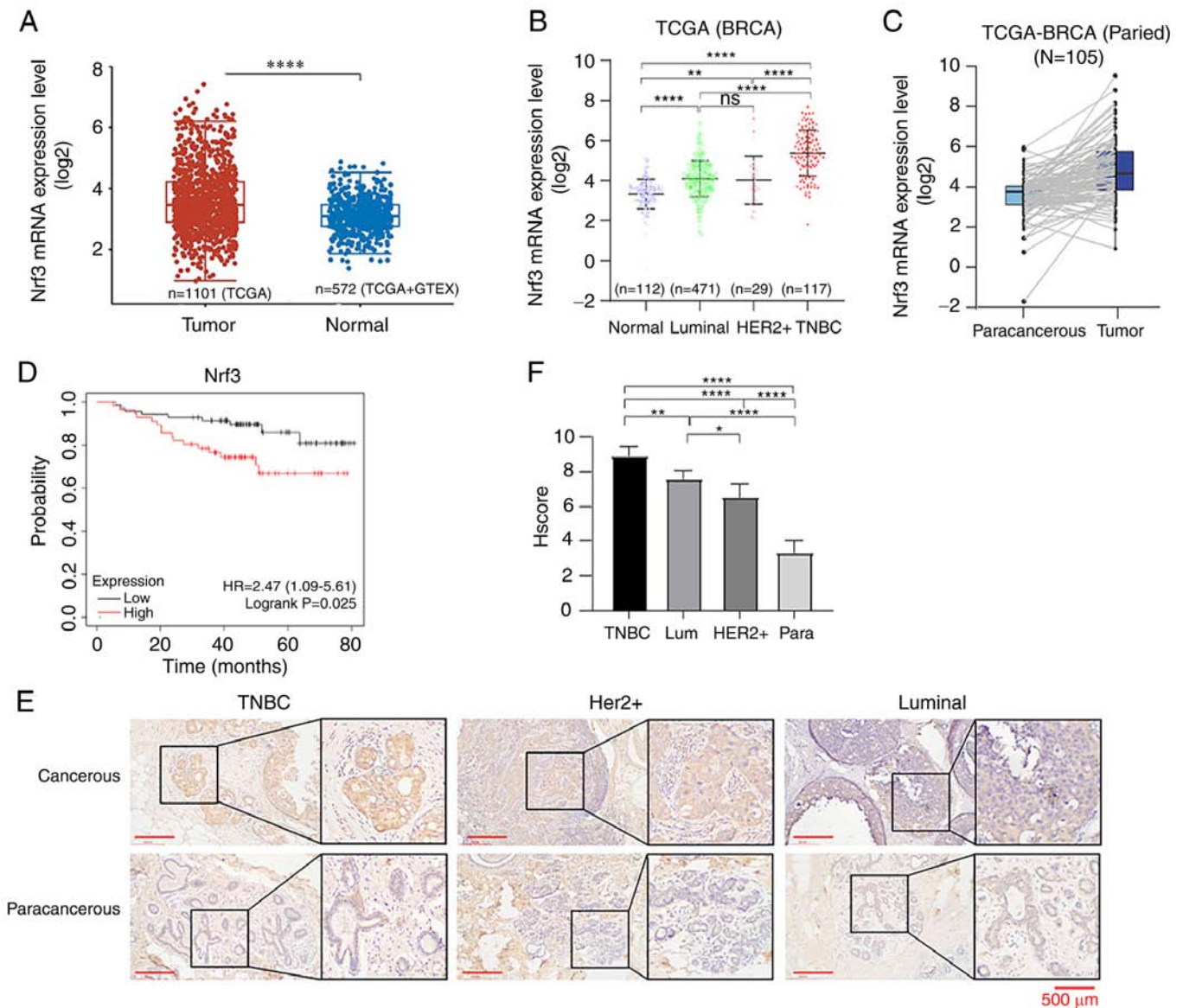


Figure 1. Nrf3 is upregulated in triple-negative breast cancer, and its expression is negatively associated with survival prognosis. (A) Differential expression of Nrf3 mRNA levels in breast cancer and the paracancerous tissues. Normal tissues, n=112; tumor tissues, n=1,066. (B) Nrf3 mRNA expression levels in normal breast tissue and different pathological types of breast cancer tissues. Normal tissues, n=112; tumor tissues, n=467; luminal, n=471; Her2⁺, n=29; TNBC, n=117. (C) Differential expression of Nrf3 mRNA levels in breast cancer and the paracancerous tissues. (D) Kaplan-Meier survival analysis between low and high Nrf3 expression breast cancer patients. Nrf3-low, n=54; Nrf3-high, n=72. P=0.025. (E) Representative images of immunohistochemical staining and the (F) immunohistochemical score in 105 breast cancer patients with different pathological types. TNBC, n=35; Her2⁺, n=35; luminal, n=35. *P<0.05, **P<0.01 and ****P<0.0001. Nrf3, nuclear factor erythroid 2-related factor 3; TNBC, triple-negative breast cancer; TCGA, The Cancer Genome Atlas; GTEx, Genotype-Tissue Expression; BRCA, breast cancer.

Overexpression and knockdown of Nrf3 were confirmed using western blotting (Fig. S2). Cells overexpressing Nrf3 were termed MDA-MB-231/Nrf3 and MDA-MB-468/Nrf3. The cells in which Nrf3 expression was knocked down were termed MDA-MB-231shNrf3#1, MDA-MB-231shNrf3#2, MDA-MB-468shNrf3#1, and MDA-MB-468shNrf3#2.

CCK-8 assays showed that overexpression of Nrf3 significantly promoted the proliferation of TNBC cells, whereas knockdown of Nrf3 reduced cell proliferation (Fig. 2). The role of Nrf3 in migration of TNBC cells was examined using wound healing and Transwell migration assays. The wound healing assays showed that the migratory rate of MDA-MB-231/Nrf3 cells increased 7.3±0.2% compared to that of MDA-MB-231,

whereas the migration rate in MDA-MB-231/shNrf3 showed a decrease of 8.2±0.15% (Fig. 2G). Additionally, the migratory rate of MDA-MB-468/shNrf3 cells decreased by 4.15±0.85% compared to that of MDA-MB-468 cells, whereas the migratory rate of MDA-MB-468/Nrf3 cells increased by 5.4±0.2% (Fig. 2H). For overexpression of Nrf3, the number of cells passing through the Transwell membranes in the different groups was 62±11 per field (MDA-MB-231), 161±17 per field (MDA-MB-231/Nrf3), 142±8.7 per field (MDA-MB-468), and 259±3.6 per field (MDA-MB-468/Nrf3) (Fig. 2E). For Nrf3 knockdown, the number of cells passing through the Transwell membranes was 82±29 per field (MDA-MB-231), 19±8.8 per field (MDA-MB-231/shRNA#1), 14±5 per field

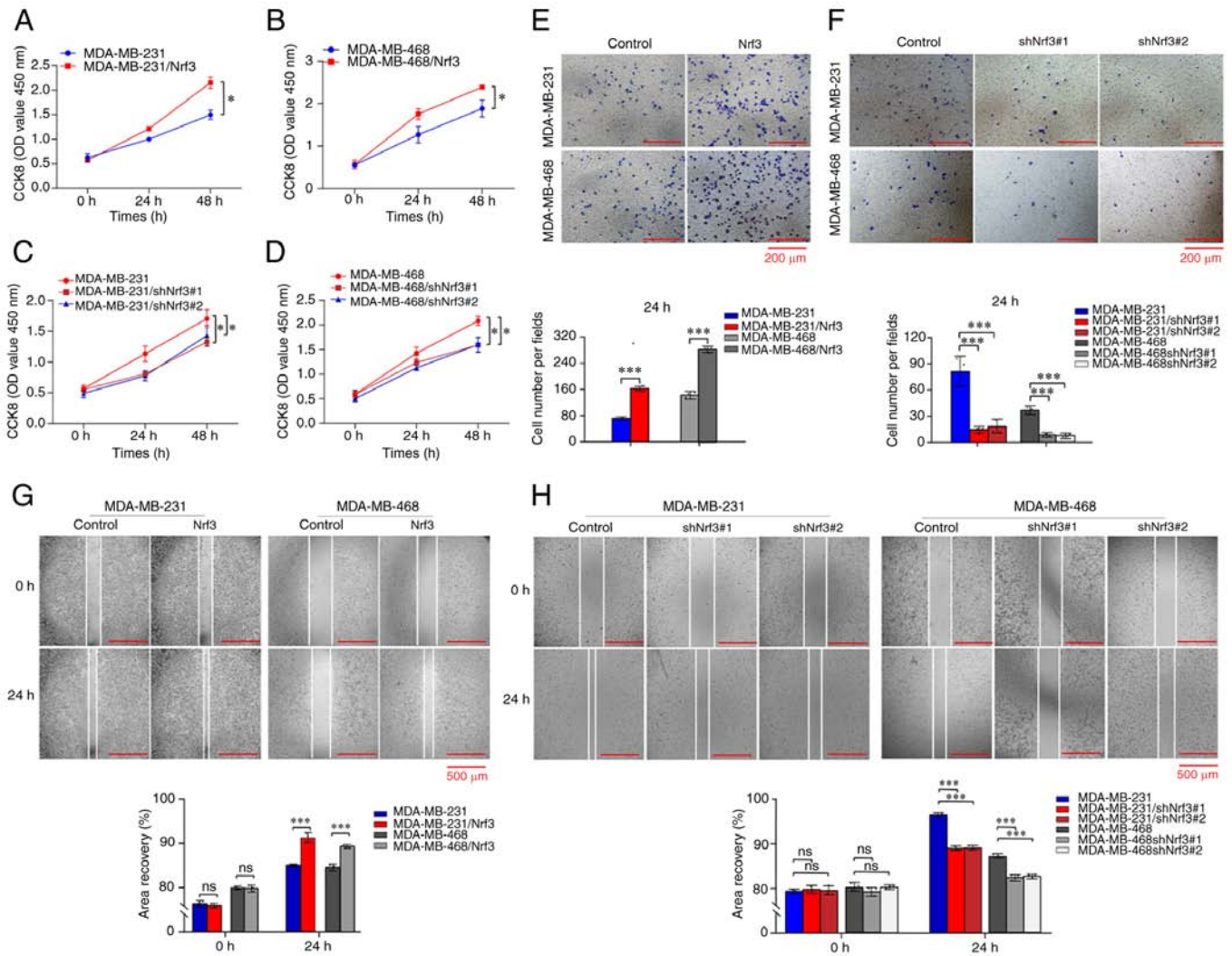


Figure 2. Overexpression of Nrf3 contributes to the proliferation and migration of TNBC, while knockdown of Nrf3 has the opposite effect. (A-D) The proliferative capacity of Nrf3 overexpression and knockdown was determined using a CCK-8 assay. (E and F) Transwell migration experiments and (G and H) wound healing assays showed that Nrf3 overexpression increased the migration of breast cancer cells, whereas Nrf3 knockdown reduced migration. *P<0.05 and ***P<0.001. Nrf3, nuclear factor erythroid 2-related factor 3; TNBC, triple-negative breast cancer; OD, optical density; sh, short hairpin.

(MDA-MB-231/shRNA#2), 42±8.7 per field (MDA-MB-468), 12±2.6 per field (MDA-MB-468/shRNA#1), and 14±3 per field (MDA-MB-468/shRNA#2) (Fig. 2F). These results demonstrated that overexpression of Nrf3 increased the invasive ability of TNBC cells, whereas knockdown of Nrf3 decreased the invasive ability of the cells.

Tumor growth and metastasis in vivo. To confirm the role of Nrf3 in promoting the proliferation and migration of TNBC *in vivo*, Nrf3-overexpression, Nrf3-knockdown MDA-MB-231, and MDA-MB-231 cells were injected. MDA-MB-231shNrf3#1 and MDA-MB-231shNrf3#2 cells failed to form subcutaneous tumors; whereas only 4 out of 5 mice developed tumors in the MDA-MB-231 group, whereas five out of five mice developed tumors in the MDA-MB-231/Nrf3 group. The average tumor weights in the different groups at the endpoint were 0.091±0.070 g (MDA-MB-231/Nrf3) and 0.017±0.007 g (MDA-MB-231) (Fig. 3A and B). Immunohistochemistry was used to detect the expression of p110α, Nrf3, E-cadherin, N-cadherin, and vimentin. The results revealed that the expression of p110α, Nrf3, N-cadherin, and vimentin in the

MDA-MB-231/Nrf3 group was substantially higher compared with the control group, whereas the expression of E-cadherin exhibited the opposite trend (Fig. 3C and D). Fig. 3E-G shows that the number of lung metastases in the different groups was as follows: 3.2±0.4 (MDA-MB-231), 4.6±0.6 (MDA-MB-231/Nrf3), 0.4±0.5 (MDA-MB-231shNrf3#1), and 0.6±0.5 (MDA-MB-231shNrf3#2). The images of the entire metastatic tumour experiment are shown in Fig. S3. These data indicated that Nrf3 facilitated the growth and migration of TNBC cells *in vivo*.

Nrf3 regulates the PI3K/AKT/mTOR pathway and expression of EMT-related proteins. To explore the underlying mechanisms of Nrf3 in enhancing the growth and invasion of breast cancer cells, transcriptome sequencing was performed using three paired biological replications of MDA-MB-231 and MDA-MB-231/Nrf3 cells. Based on the sequencing data, 215 significantly differentially expressed genes, including 159 upregulated and 66 downregulated genes (Fig. S4). GSEA showed that EMT-related genes were enriched, which is a critical mechanism for cancer metastasis (Fig. 4A). The genes

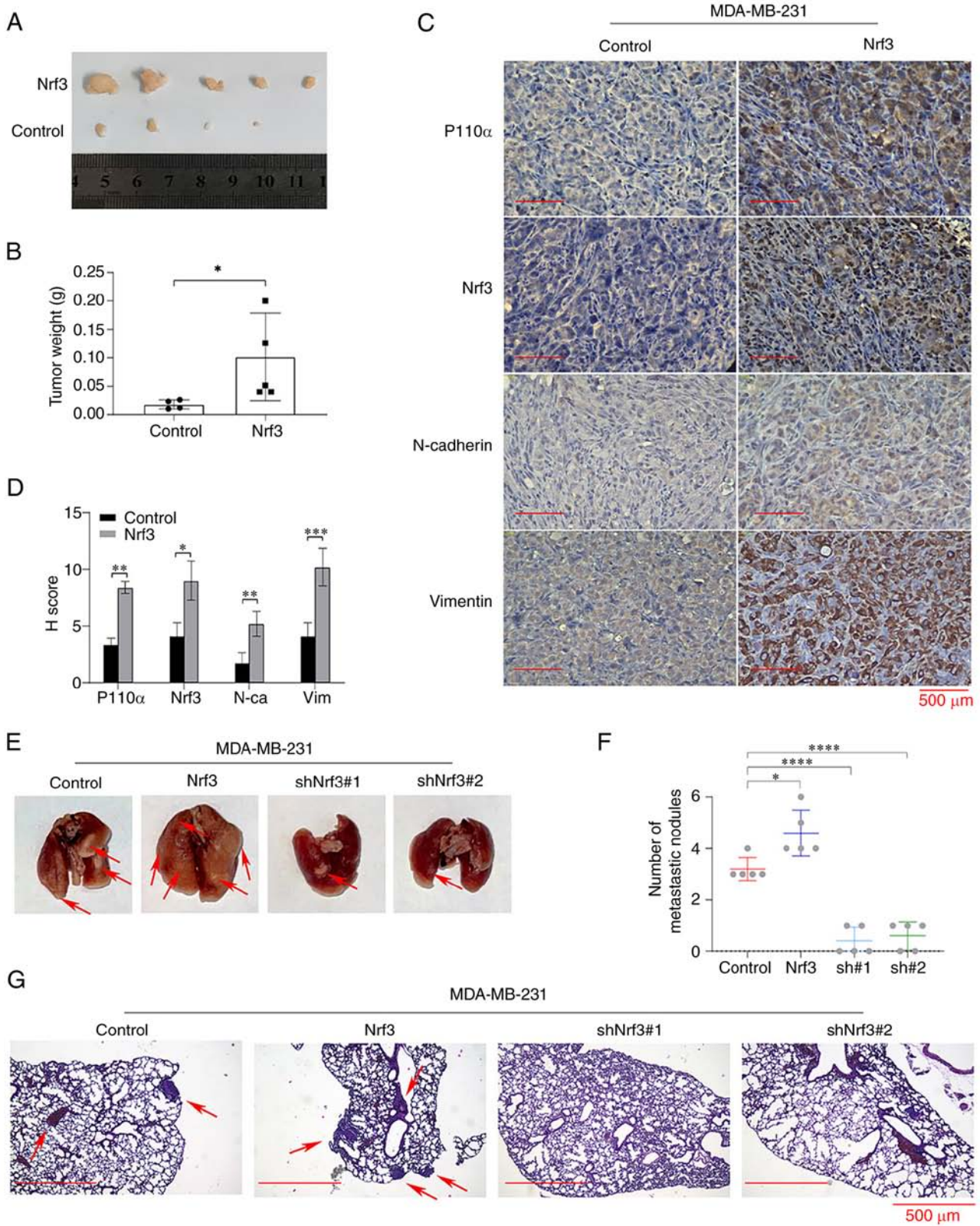


Figure 3. Nrf3 promotes TNBC cell proliferation and metastasis *in vivo*. (A) Representative images of tumors in the different groups. (B) Mean tumor weight in each group. (C) p110 α , Nrf3, N-cadherin, and vimentin expression were detected by immunostaining in the xenografted tumors. Magnification, x400. (D) Mean staining intensity of p110 α , Nrf3, N-cadherin, and vimentin (E) Representative images of the lungs excised from the mice in the different groups. (F) The number of metastatic lung sites (indicated by arrows) was counted. Data are presented as the mean \pm SEM of 5 repeats. (G) Representative images of H&E-stained sections in the dissected lungs 60 days after inoculation. Magnification, x100. * $P < 0.05$, ** $P < 0.01$, *** $P < 0.001$ and **** $P < 0.0001$. Nrf3, nuclear factor erythroid 2-related factor 3; TNBC, triple-negative breast cancer; sh, short hairpin; N-ca, N-Cadherin; Vim, Vimentin.

related to proliferation and migration were clustered and are displayed using thermography (Fig. 4B). To validate this

result, RT-qPCR was used to examine the mRNA levels of the above-related genes (p110 α , MMP3, MMP9, TGF β 1, TGF

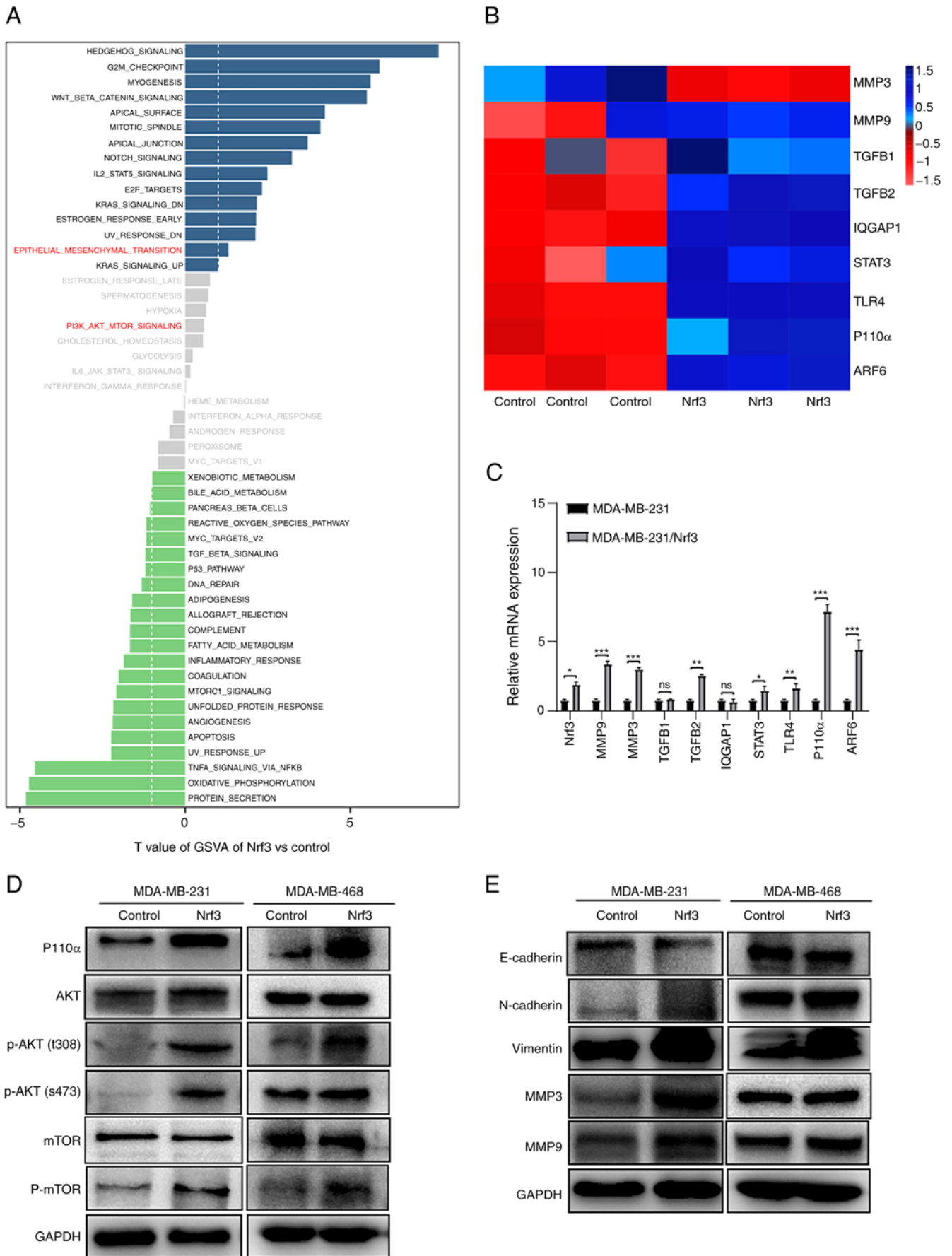


Figure 4. Nrf3 regulates PI3K/AKT/mTOR signaling and EMT-related protein expression. (A). Gene set variation Analysis was performed based on RNA sequencing data. (B) The genes related to proliferation and migration were clustered and displayed as a heat map. (C) quantitative PCR was used to verify the relative expression levels of EMT-related genes normalized to actin. (D) Western blot analysis showed the relative expression of the proteins in the PI3k/Akt/mTOR pathway. (E) Relative expression of EMT-related proteins. * $P < 0.05$, ** $P < 0.01$ and *** $P < 0.001$.

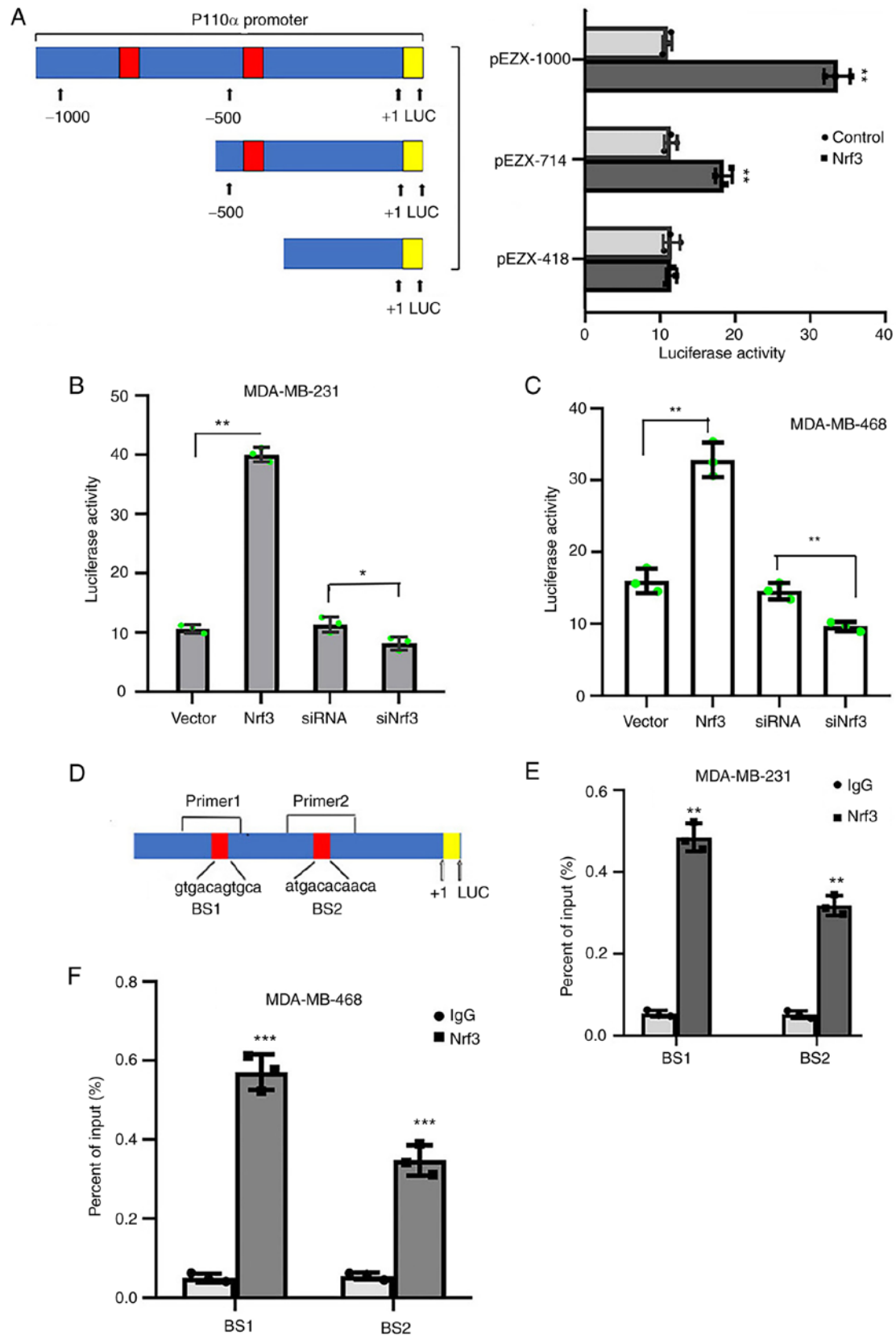


Figure 5. Nrf3 directly bound to the promoter region of P110 α . (A) Schematic representation of the structures of the P110 α promoter-luciferase constructs. Briefly, 1kb DNA and 5' truncated fragments of the P110 α promoter upstream of the transcription start sites were inserted into the luciferase reporter vector pEZX in the sense orientation. Full-length promoter vector (pEZX-1000), and deletion mutation reporters (pEZX-714 and pEZX-418) with or without an Nrf3 expression vector, were co-transfected into MDA-MB-231 cells. (B and C) MDA-MB-231 and MDA-MB-468 cells were co-transfected with pEZX-1000 and an Nrf3 expression vector or a control vector and Nrf3 siRNA (si-Nrf3) or control siRNA. The promoter activity in the cells was examined using a dual luciferase assay. (D) Nrf3 putative binding sites in the P110 α promoter and primers used in the ChIP assay. (E and F) Results from the ChIP assay conducted using chromatin isolated from MDA-MB-231 and MDA-MB-468 cells transfected with Nrf3 overexpression or a control plasmid; IgG isotype control was used as the negative control; 1% of the total cell lysates were subjected to PCR before immunoprecipitation (input control). Data are presented as the mean \pm SD of three independent experiments. *P<0.05, **P<0.01 and ***P<0.001. Nrf3, nuclear factor erythroid 2-related factor 3; siRNA, small interfering RNA; BS, binding sites.

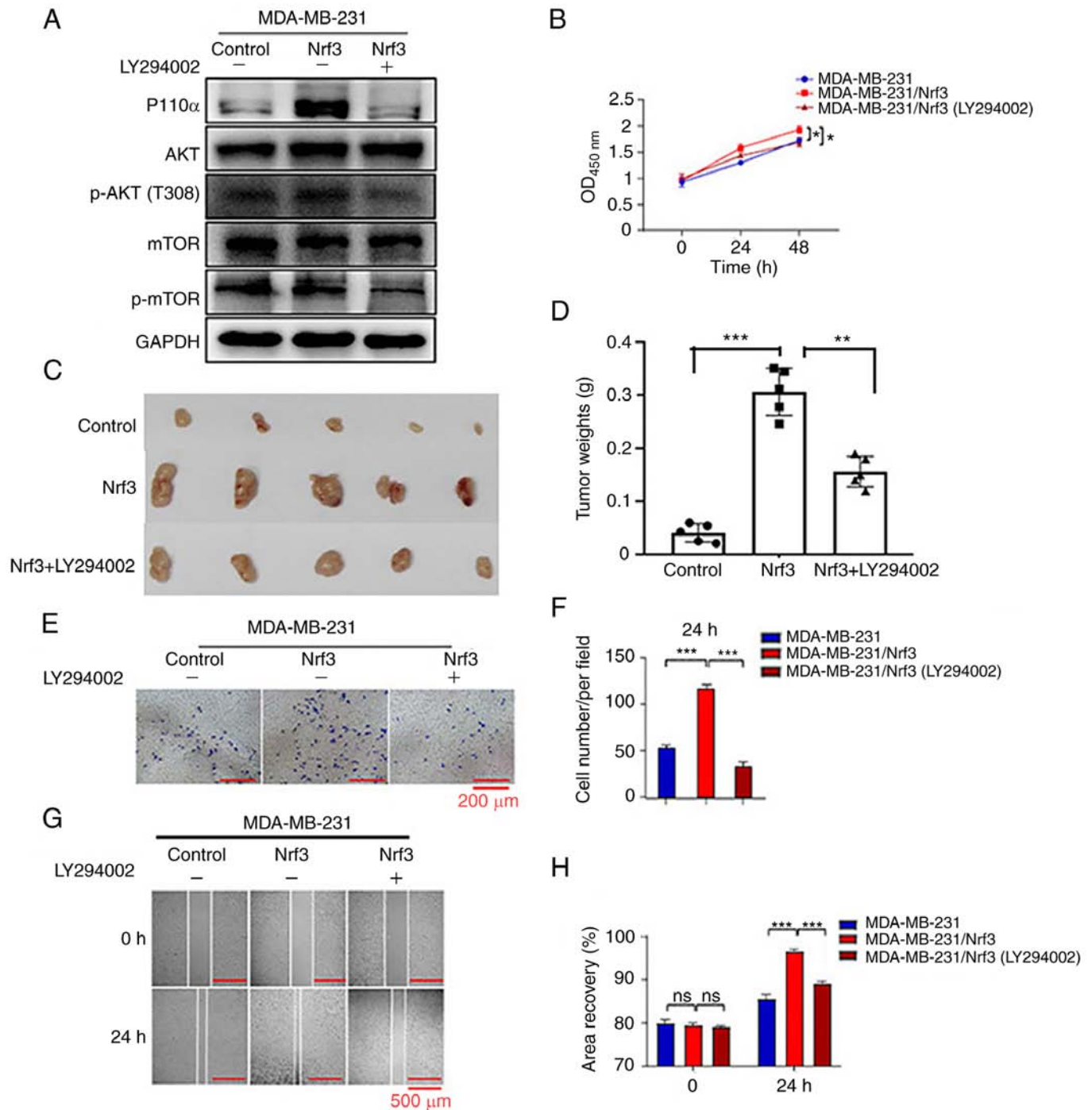


Figure 6. PI3K inhibitor partly reverses the proliferation and migration of Nrf3 overexpressing triple-negative breast cancer cells. (A) P110 α , AKT, P-AKT, mTOR, and p-mTOR expression following treatment with the PI3K inhibitor. (B-D) CCK-8 assays and animal experiments showed that the proliferative ability of MDA-MB-231/Nrf3 cells was partly reduced when treated with the PI3K inhibitor. The migratory capacity was detected using (E and F) Transwell migration assays and (G and H) wound healing assays. The results suggest PI3K inhibitor partly reverses the effect of Nrf3 on migration in MDA-MB-231 cells. * $P < 0.05$, ** $P < 0.01$ and *** $P < 0.001$. Nrf3, nuclear factor erythroid 2-related factor 3; OD, optical density.

$\beta 2$, IQGAP1, STAT3, TLR4, and ARF6). The most significant change among these candidate molecules was in p110 α in the MDA-MB-231/Nrf3 cell line compared with MDA-MB-231 cells (Fig. 4C), which was consistent with transcriptome sequencing. Additionally, the expression of the p110 α protein and its downstream molecules were further determined by western blotting. Comparing the Nrf3 overexpression group with the control group revealed that p-AKT and p-mTOR

expression was increased. However, the expression of AKT and mTOR were not significantly altered (Fig. 4D). Furthermore, owing to Nrf3 overexpression, N-cadherin, vimentin, MMP3, and MMP9 expression increased, whereas E-cadherin expression decreased (Fig. 4E).

Nrf3 directly binds to the p110 α promoter and increases its expression. A p110 α promoter was subcloned into the pEZX

vector to determine whether Nrf3 regulated p110 α expression in TNBC cells. The full-length reporter plasmid was designated pEZX-1000, which contained two predicted Nrf3 binding sites (-725 to -715 and -429 to -419). Additionally, two deletion mutation reporters were constructed using this plasmid (pEZX-714 and pEZX-418). pEZX-1000, pEZX-714, and pEZX-418 plasmids were co-transfected with the Nrf3 expression vector into the MDA-MB-231 cells. The results showed that Nrf3 enhanced the activity of the full-length reporter (pEZX-1000) and the deletion mutant reporter (pEZX-714), whereas the other deletion mutant reporter (pEZX-418) did not exhibit the same activity (Fig. 5A). Further, MDA-MB-231 and MDA-MB-468 cells were co-transfected with pEZX-1000 and an Nrf3 expression vector or siRNA Nrf3 (Fig. 5B and C) showed that overexpression of Nrf3 enhanced p110 α promoter activity. Conversely, Nrf3 knockdown attenuated the p110 α promoter activity.

A ChIP assay was performed in MDA-MB-231 and MDA-MB-468 cells to determine the mutual interactions between Nrf3 and potential Nrf3-binding sites in the p110 α promoter region. Primers were located at binding sites 1 (BS1) and 2 (BS2) of the p110 α promoter (Fig. 5D). An anti-Nrf3 antibody immunoprecipitated significantly more chromatin in MDA-MB-231/Nrf3 and MDA-MB-468/Nrf3 cells compared with the control (Fig. 5E and F). These results suggest that Nrf3 directly binds to the p110 α promoter region and affects the transcriptional activity of p110 α in MDA-MB-231 and MDA-MB-468 cells.

PI3K inhibitor partly reverses the effects of Nrf3 overexpression. MDA-MB-231/Nrf3 cells were used for the recovery experiments. Western blot analysis was performed after cells were treated with the PI3K inhibitor, LY294002, (Fig. 6A). The CCK-8 assays and animal experiments showed that the PI3K inhibitor partly reversed the proliferation of MDA-MB-231/Nrf3 cells *in vitro* and *in vivo* (Fig. 6B-D). As measured by wound healing and Transwell assays, the PI3K inhibitor attenuated the effect of Nrf3, resulting in the migration of MDA-MB-231 cells (Fig. 6E-H). Based on these findings, PI3K may be involved in regulating Nrf3-mediated proliferation and migration in breast cancer cells.

Discussion

In the present study, Nrf3 was shown to play a critical role in the proliferation and invasion of TNBC cells via the PI3K/AKT/mTOR signaling pathway. First, Nrf3 expression was evidently upregulated in TNBC tissues compared with the noncancerous tissues, and its expression was associated with worse survival times. Additionally, overexpression of Nrf3 was shown to significantly enhance cell proliferation and migration *in vitro* and *in vivo*, while Nrf3 knockdown produced the opposite results. Moreover, Nrf3 activated the PI3K/AKT signaling pathway and regulated EMT-related protein expression. Luciferase and ChIP assays showed that Nrf3 positively regulated PI3K expression. By inhibiting PI3K, the effect of Nrf3 on cell growth and invasion was partially reversed.

Nrf3 is associated with the development and occurrence of several types of cancer (33-35), and its function remains contested. Chevillard *et al* (36) suggested that Nrf3 has a protective effect in lymphoma; however, further validation at the molecular level is lacking. Other reports have shown that

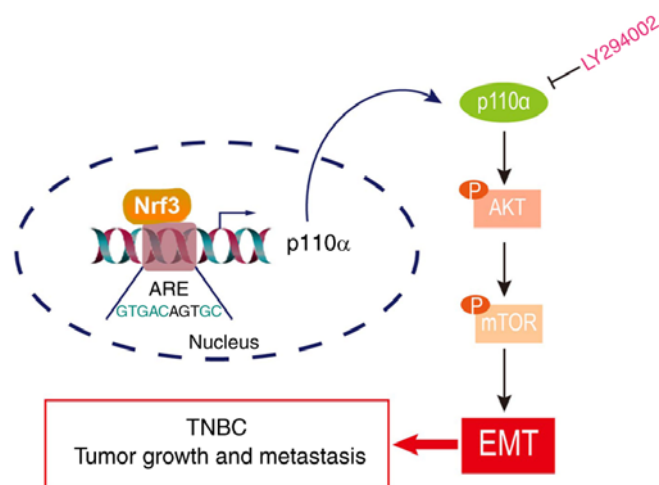


Figure 7. Schematic showing how Nrf3 promotes the proliferation and metastasis of triple-negative breast cancer. Nrf3, nuclear factor erythroid 2-related factor 3; EMT, epithelial-mesenchymal transition.

Nrf3 may act as an oncogene to promote carcinogenesis, such as in colon cancer (17), bladder cancer (18), and hepatocellular carcinoma (37). Therefore, Nrf3 can function as both an oncogene or tumor suppressor gene dependent on the type of cancer. The results of the present study showed that Nrf3, as an oncogene, increased the proliferation and migration of TNBC cells *in vitro* and *in vivo*. Although Nrf3 expression was previously reported to be reduced in breast cancer (38), the results of the present study demonstrated that Nrf3 expression in TNBC was higher than in adjacent tissues and other cancer types. These differences in research findings may be attributed to differences in sample sizes and tumor types.

The underlying mechanism of Nrf3 in promoting proliferation and migration may involve the PI3K/AKT/mTOR signaling pathway. The genes related to proliferation and migration were determined using transcriptome sequencing and qPCR. The results of the present study showed that p110 α expression was most notably altered among the candidate molecules. p110 α is the second most frequently mutated gene in TNBC (39) and plays an important role in regulating receptor tyrosine kinase (RTK) signaling, cell growth, the cell cycle, and cell survival in breast cancer (40). Expression of p110 α and its downstream molecules was also detected. The PI3K/AKT/mTOR signaling pathway was activated by Nrf3, which may be essential for the multiple cellular activities observed (41), including cell metabolism, cell growth and migration, and apoptosis. Hyperactivation of PI3K/AKT/mTOR promotes cell growth and migration of TNBC cells (42). Moreover, using the luciferase reporter and ChIP assays, it was found that Nrf3 directly bound to the p110 α promoter sequence. To the best of our knowledge, this is the first study to show that Nrf3 is responsible for the activation of p110 α transcription.

During cancer metastasis, EMT also plays an important role. EMT is characterized by the loss of epithelial markers, an increase in mesenchymal markers, and increased cell migration (43,44). Activation of EMT has been shown to promote the phenotypic association of proliferative migration, tumor induction, stem cell activity of tumor cells, and tumor drug resistance

in breast cancer (45). Nrf3 knockdown reduces the migration of hepatocellular carcinoma cells by inhibiting EMT (46). The present study showed that the overexpression of Nrf3 upregulated N-cadherin and vimentin expression whilst reducing E-cadherin expression. In contrast, p110 α also triggered EMT by inducing the loss of E-cadherin (42). Thus, it is hypothesized that Nrf3 activated EMT via PI3K/AKT/mTOR signaling, although the precise mechanism still requires further investigation.

The present study first revealed that Nrf3 promoted the growth and migration of TNBC cells *in vitro* and *in vivo*. Additionally, it was found that Nrf3 increased p110 α , p-AKT, and p-mTOR expression and regulated EMT expression-related proteins. Luciferase reporter and ChIP assays showed that Nrf3 increased p110 α promoter activity by directly binding to the promoter region. A link between Nrf3 and p110 α indicated that Nrf3-mediated proliferation and migration of TNBC may be related to PI3K/AKT/mTOR signaling (Fig. 7).

In conclusion, the present study results demonstrated that Nrf3 facilitates the proliferation and migration of TNBC by activating PI3K/AKT/mTOR signaling and EMT, thereby providing a potential novel therapeutic target for TNBC.

Acknowledgements

Not applicable.

Funding

This study was supported by the Strategic Cooperation Research Project of Nan Chong (grant no. 20SXEXTD004) and the Major Emphasis Project of North of Sichuan Medical College (grant no. CBY22-ZDA02, CBY22-ZD04).

Availability of data and materials

Transcriptome sequencing datasets generated and/or analyzed during the current study are available in the Sequence Read Archive database (<https://www.ncbi.nlm.nih.gov/sra>) as submission number PRJNA965920. The other datasets used and/or analyzed during the present study are available from the corresponding author on reasonable request.

Authors' contributions

JCT, QYH, WMC and WH designed the study, performed the experiments and wrote the manuscript. YHC and MWC performed the statistical analysis. JCT, QYH and WMC confirm the authenticity of all the raw data. All authors have read and approved the final manuscript.

Ethics approval and consent to participate

In accordance with the guidelines of the Animal Protection Law of the People's Republic of China-2009, procedures on animals were approved by the Affiliated Hospital of North Sichuan Medical College (approval no. 2022033).

Patient consent for publication

Not applicable.

Competing interests

The authors declare that they have no competing interests.

References

- Sung H, Ferlay J, Siegel RL, Laversanne M, Soerjomataram I, Jemal A and Bray F: Global Cancer Statistics 2020: GLOBOCAN estimates of incidence and mortality worldwide for 36 cancers in 185 countries. *CA Cancer J Clin* 71: 209-249, 2021.
- Perou CM, Sørliie T, Eisen MB, van de Rijn M, Jeffrey SS, Rees CA, Pollack JR, Ross DT, Johnsen H, Akslen LA, *et al*: Molecular portraits of human breast tumours. *Nature* 406: 747-752, 2000.
- Brown M, Tsodikov A, Bauer KR, Parise CA and Caggiano V: The role of human epidermal growth factor receptor 2 in the survival of women with estrogen and progesterone receptor-negative, invasive breast cancer: The California Cancer Registry, 1999-2004. *Cancer* 112: 737-747, 2008.
- Duffy MJ, McGowan PM and Crown J: Targeted therapy for triple-negative breast cancer: Where are we? *Int J Cancer* 131: 2471-2477, 2012.
- Gradishar WJ, Anderson BO, Abraham J, Aft R, Agnese D, Allison KH, Blair SL, Burstein HJ, Dang C, Elias AD, *et al*: Breast cancer, version 3.2020, NCCN clinical practice guidelines in oncology. *J Natl Compr Canc Netw* 18: 452-478, 2020.
- Kobayashi A, Ito E, Toki T, Kogame K, Takahashi S, Igarashi K, Hayashi N and Yamamoto M: Molecular cloning and functional characterization of a new Cap'n' collar family transcription factor Nrf3. *J Biol Chem* 274: 6443-6452, 1999.
- Motohashi H, O'Connor T, Katsuoka F, Engel JD and Yamamoto M: Integration and diversity of the regulatory network composed of Maf and CNC families of transcription factors. *Gene* 294: 1-12, 2002.
- Sekine H and Motohashi H: Roles of CNC transcription factors NRF1 and NRF2 in cancer. *Cancers (Basel)* 13: 541, 2021.
- Yuan J, Zhang S and Zhang Y: Nrf1 is paved as a new strategic avenue to prevent and treat cancer, neurodegenerative and other diseases. *Toxicol Appl Pharmacol* 360: 273-283, 2018.
- Rojo de la Vega M, Chapman E and Zhang DD: NRF2 and the hallmarks of cancer. *Cancer Cell* 34: 21-43, 2018.
- Derjuga A, Gourley TS, Holm TM, Heng HH, Shivdassani RA, Ahmed R, Andrews NC and Blank V: Complexity of CNC transcription factors as revealed by gene targeting of the Nrf3 locus. *Mol Cell Biol* 24: 3286-3294, 2004.
- He F, Ru X and Wen T: NRF2, a transcription factor for stress response and beyond. *Int J Mol Sci* 21: 4777, 2020.
- Radhakrishnan SK, Lee CS, Young P, Beskow A, Chan JY and Deshaies RJ: Transcription factor Nrf1 mediates the proteasome recovery pathway after proteasome inhibition in mammalian cells. *Mol Cell* 38: 17-28, 2010.
- Kobayashi A: Roles of NRF3 in the hallmarks of cancer: Proteasomal inactivation of tumor suppressors. *Cancers (Basel)* 12: 2681, 2020.
- Braun S, Hanselmann C, Gassmann MG, Auf Dem Keller U, Born-Berclaz C, Chan K, Kan YW and Werner S: Nrf2 transcription factor, a novel target of keratinocyte growth factor action which regulates gene expression and inflammation in the healing skin wound. *Mol Cell Biol* 22: 5492-5505, 2002.
- Pepe AE, Xiao Q, Zampetaki A, Zhang Z, Kobayashi A, Hu Y and Xu Q: Crucial role of nrf3 in smooth muscle cell differentiation from stem cells. *Circ Res* 106: 870-979, 2010.
- Bury M, Le Calvé B, Lessard F, Dal Maso T, Saliba J, Michiels C, Ferbeyre G and Blank V: NFE2L3 controls colon cancer cell growth through regulation of DUX4, a CDK1 inhibitor. *Cell Rep* 29: 1469-1481.e9, 2019.
- Qian J, Huang C, Zhu Z, He Y, Wang Y, Feng N, He S, Li X, Zhou L, Zhang C and Gong Y: NFE2L3 promotes tumor progression and predicts a poor prognosis of bladder cancer. *Carcinogenesis* 43: 457-468, 2022.
- Waku T, Nakamura N, Koji M, Watanabe H, Katoh H, Tatsumi C, Tamura N, Hatanaka A, Hirose S, Katayama H, *et al*: NRF3-POMP-20S proteasome assembly axis promotes cancer development via ubiquitin-independent proteolysis of p53 and retinoblastoma protein. *Mol Cell Biol* 40: e00597-19, 2020.
- Yin L, Duan JJ, Bian XW and Yu SC: Triple-negative breast cancer molecular subtyping and treatment progress. *Breast Cancer Res* 22: 61, 2020.

21. Katso R, Okkenhaug K, Ahmadi K, White S, Timms J and Waterfield MD: Cellular function of phosphoinositide 3-kinases: Implications for development, homeostasis, and cancer. *Annu Rev Cell Dev Biol* 17: 615-675, 2001.
22. Engelman JA, Luo J and Cantley LC: The evolution of phosphatidylinositol 3-kinases as regulators of growth and metabolism. *Nat Rev Genet* 7: 606-619, 2006.
23. Gjelijaj E and Hamel PA: Distinct epithelial-to-mesenchymal transitions induced by PIK3CA (H1047R) and PIK3CB. *J Cell Sci* 134: jcs248294, 2021.
24. Grille SJ, Bellacosa A, Upson J, Klein-Szanto AJ, van Roy F, Lee-Kwon W, Donowitz M, Tsiachlis PN and Larue L: The protein kinase Akt induces epithelial mesenchymal transition and promotes enhanced motility and invasiveness of squamous cell carcinoma lines. *Cancer Res* 63: 2172-2178, 2003.
25. Cai BQ, Chen WW, Zhao JA, Hou W and Tang JC: Nrf3 Promotes 5-FU resistance in colorectal cancer cells via the NF- κ B/BCL-2 signaling pathway in vitro and in vivo. *J Oncol* 2021: 9355555, 2021.
26. Bolger AM, Lohse M and Usadel B: Trimmomatic: A flexible trimmer for Illumina sequence data. *Bioinformatics* 30: 2114-2120, 2014.
27. Kim D, Langmead B and Salzberg SL: HISAT: A fast spliced aligner with low memory requirements. *Nat Methods* 12: 357-360, 2015.
28. Trapnell C, William BA, Pertea G, AMortazavi A, Kwan G, van Baren MJ, Salzberg SL, Wold BJ and Pachter L: Transcript assembly and quantification by RNA-Seq reveals unannotated transcripts and isoform switching during cell differentiation. *Nat Biotechnol* 28: 511-515, 2010.
29. Anders S, Pyl PT and Huber W: HTSeq-a Python framework to work with high-throughput sequencing data. *Bioinformatics* 31: 166-169, 2015.
30. Anders S and Huber W: Differential expression of RNA-Seq data at the gene level-the DESeq package. EMBL, 2013.
31. Hännelmann S, Castelo R and Guinney J: GSEA: Gene set variation analysis for microarray and RNA-seq data. *BMC Bioinformatics* 14: 7, 2013.
32. Livak KJ and Schmittgen TD: Analysis of relative gene expression data using real-time quantitative PCR and the 2(-Delta Delta C(T)) method. *Methods* 25: 402-408, 2001.
33. Chowdhury A, Katoh H, Hatanaka A, Iwanari H, Nakamura N, Hamakubo T, Natsume T, Waku T and Kobayashi A: Multiple regulatory mechanisms of the biological function of NRF3 (NFE2L3) control cancer cell proliferation. *Sci Rep* 7: 12494, 2017.
34. Immonen A, Haapasaari KM, Skarp S, Karihtala P and Teppo HR: NRF3 decreases during melanoma carcinogenesis and is an independent prognostic marker in melanoma. *Oxid Med Cell Longev* 2022: 2240223, 2022.
35. Waku T, Katayama H, Hiraoka M, Hatanaka A, Nakamura N, Tanaka Y, Tamura N, Watanabe A and Kobayashi A: NFE2L1 and NFE2L3 complementarily maintain basal proteasome activity in cancer cells through CPEB3-mediated translational repression. *Mol Cell Biol* 40: e00010-20, 2020.
36. Chevillard G, Paquet M and Blank V: Nfe2l3 (Nrf3) deficiency predisposes mice to T-cell lymphoblastic lymphoma. *Blood* 117: 2005-2008, 2011.
37. Yu MM, Feng YH, Zheng L, Zhang J and Luo GH: Short hairpin RNA-mediated knockdown of nuclear factor erythroid 2-like 3 exhibits tumor-suppressing effects in hepatocellular carcinoma cells. *World J Gastroenterol* 25: 1210-1223, 2019.
38. Sun J, Zheng Z, Chen Q, Pan Y, Lu H, Zhang H, Yu Y and Dai Y: NRF3 suppresses breast cancer cell metastasis and cell proliferation and is a favorable predictor of survival in breast cancer. *Oncotargets Ther* 12: 3019-3030, 2019.
39. Xie G, Ji A, Yuan Q, Jin Z, Yuan Y, Ren C, Guo Z, Yao Q, Yang K, Lin X and Chen L: Tumour-initiating capacity is independent of epithelial-mesenchymal transition status in breast cancer cell lines. *Br J Cancer* 110: 2514-2523, 2014.
40. Tang Y, Wang S, Li Y, Yuan C, Zhang J, Xu Z, Hu Y, Shi H and Wang S: Simultaneous glutamine metabolism and PD-L1 inhibition to enhance suppression of triple-negative breast cancer. *J Nanobiotechnology* 20: 216, 2022.
41. Miricescu D, Totan A, Stanescu-Spinu II, Badoiu SC, Stefani C and Greabu M: PI3K/AKT/mTOR signaling pathway in breast cancer: From molecular landscape to clinical aspects. *Int J Mol Sci* 22: 173, 2020.
42. Costa RLB, Han HS and Gradishar WJ: Targeting the PI3K/AKT/mTOR pathway in triple-negative breast cancer: A review. *Breast Cancer Res Treat* 169: 397-406, 2018.
43. Aiello NM and Kang Y: Context-dependent EMT programs in cancer metastasis. *J Exp Med* 216: 1016-1026, 2019.
44. Chaffer CL, San Juan BP, Lim E and Weinberg RA: EMT, cell plasticity and metastasis. *Cancer Metastasis Rev* 35: 645-654, 2016.
45. Bobal P, Lastovickova M and Bobalova J: The Role of ATRA, natural ligand of retinoic acid receptors, on EMT-related proteins in breast cancer: Minireview. *Int J Mol Sci* 22: 13345, 2021.
46. Ren YG, Wang YJ, Hao S, Yang YH, Xiong WD and Qiu L: NFE2L3 promotes malignant behavior and EMT of human hepatocellular carcinoma (HepG2) cells via Wnt/ β -catenin pathway. *J Cancer* 11: 6939-6949, 2020.



Copyright © 2023 Chen et al. This work is licensed under a Creative Commons Attribution-NonCommercial-NoDerivatives 4.0 International (CC BY-NC-ND 4.0) License.